Temperature dependence of bifurcation of equilibria in the SU(2) Lipkin model

1994 J. Phys. A: Math. Gen. 27 697

(http://iopscience.iop.org/0305-4470/27/3/015)

J. Phys. A: Math. Gen. 27 (1994) 697–713. Printed in the UK

Temperature dependence of bifurcation of equilibria in the $SU(2)$ Lipkin model*

M O Terra†, A H Blin‡, B Hiller‡, M C Nemes§, C Providência‡ and J da Providência‡

† Instituto de Física, Departamento de Física-Matemática, Universidade de São Paulo, CP 20516, São Paulo, SP, Brazil

‡ Centro de Física Teórica (INIC), Universidade de Coimbra, P-3000 Coimbra, Portugal

§ Departamento de Física, Instituto de Ciências Exatas, Universidade Federal de Minas Gerais, CP 702, 31270 Belo Horizonte, MG, Brazil

Received 27 August 1993

Abstract. We present a detailed analysis of the thermodynamical properties as well as thermal effects on the classical dynamics of the $SU(2)$ Lipkin model. Particular attention is devoted to the temperature dependence of fixed points and bifurcation of equilibria. We find that qualitatively, temperature effects tend to counterbalance the effects of the two-body interaction.

1. Introduction

The $SU(2)$ Lipkin model was originally proposed as an exactly soluble model which contains the main characteristics of the nuclear two-body interaction [1]. Therefore, it constitutes a powerful tool in what concerns the study of the validity of the various many-body approximation schemes used to describe nuclear spectra. In this context one is usually concerned with ground states or low-lying energy-level properties.

Recently the $SU(2)$ Lipkin model, due to its very rich and simple structure, has been revisited by various groups in the context of dynamical systems. Its semiclassical limit has been studied by several authors [2, 3], however omitting the second interaction term ($W = 0$ in (1)). In the particular case of the Lipkin model, the classical limit is mathematically well defined and unique. Also $1/N$, where N is the number of particles can be considered as an expansion parameter [4].

In our opinion one of the important open questions in the area of dynamical systems is the effect of temperature. The purpose of the present paper is to shed some light on this question by presenting a detailed analysis of both thermodynamical properties, phase transition with temperature and the thermal dynamics properties: the behaviour of fixed points and bifurcation of equilibria as a function of temperature in the most general version of the model are presented. We find that qualitatively speaking the effect of temperature is to render the system weakly coupled. It counterbalances the effect of the coupling parameters.

This study is performed as follows: in section 2 we present the model and in section 3 the thermodynamical properties are derived in the mean-field approximation. Next, the dynamical effects of temperature are presented in section 4. Concluding remarks are given in section 5.

* Work partially supported by CNPq and FAPESP.

0305-4470/94/030697+17$07.50

2. The model

As originally proposed by Lipkin, Meshkov and Glick the $SU(2)$ Lipkin model consists of an N-fermion system occupying a two N-fold degenerated levels with energies $+\frac{1}{2}\epsilon$ and $-\frac{1}{2}\epsilon$ respectively. Each state is described by a quantum number σ which has the value $+1$ (-1) in the upper (lower) shell. The other quantum number p specifies the particular degenerate state within the shell.

The Hamiltonian is constructed as follows:

$$H = \tfrac{1}{2}\epsilon \sum_{\sigma=\pm 1}\sum_{p=1}^{N} \sigma a_{p\sigma}^{\dagger} a_{p\sigma} - \tfrac{1}{2}V \sum_{\sigma=\pm 1}\sum_{p=1}^{N}\sum_{p'=1}^{N} a_{p\sigma}^{\dagger} a_{p'\sigma}^{\dagger} a_{p'-\sigma} a_{p-\sigma}$$

$$- \tfrac{1}{2}W \sum_{\sigma=\pm 1}\sum_{p=1}^{N}\sum_{p'=1}^{N} a_{p\sigma}^{\dagger} a_{p'-\sigma}^{\dagger} a_{p'\sigma} a_{p-\sigma} \tag{1}$$

where the operators $a_{p\sigma}^{\dagger}(a_{p\sigma})$ correspond to the creation (annihilation) of a particle in the p state of the σ level. V and W are the parameters specifying the strength of the interactions: the V term mixes states having different numbers of excited particle–hole pairs, by scattering a pair of particles in the same level to the other level. The W term does not mix configurations and simultaneously scatters one particle up and the other down. Introducing the following quasi-spin $SU(2)$ operators:

$$J_z = \tfrac{1}{2}\sum_{p=1}^{N}\left[a_{p+1}^{\dagger} a_{p+1} - a_{p-1}^{\dagger} a_{p-1}\right] \tag{2}$$

$$J_+ = J_-^{\dagger} = \sum_{p=1}^{N} a_{p+1}^{\dagger} a_{p-1}\,. \tag{3}$$

The Hamiltonian can be cast into the form [1]

$$H = \epsilon J_z - \tfrac{1}{2}V(J_+^2 + J_-^2) - \tfrac{1}{2}W(J_+J_- + J_-J_+)\,. \tag{4}$$

The Casimir operator of the group J^2 commutes with H and represents half of the total numbers of particles $N/2$.

3. Thermodynamics

When one considers a finite number of particles the thermodynamics of the model can only be studied numerically. In the large-N limit, however, ($J \to \infty$, $\hbar \to 0$, $\hbar J$ finite) the mean-field approximation becomes exact and the thermodynamic properties of the model can be obtained almost analytically. In the present section we start by constructing the equilibrium state in a variational mean-field approach. The relevant thermodynamic quantities are then calculated, with particular emphasis on their phase transition behaviour.

3.1. Equilibrium states

The most general form of a mean-field density matrix for the model under consideration is the following:

$$\hat{D}_0 = K \exp(-\beta h_{\mathrm{MF}}) \tag{5}$$

where

$$h_{\mathrm{MF}} = \alpha_1 J_z + \alpha_2 J_+ + \alpha_2^* J_- \tag{6}$$

and K is a normalization constant. The set of complex parameters α_i are viewed by imposing that the free energy is a minimum,

$$\beta F = \beta \operatorname{Tr}(D_0 H) + \operatorname{Tr}(D_0 \ln D_0) \tag{7}$$

where β is related to the temperature as $\beta = 1/k_{\mathrm{B}}T$. It is, however, much simpler to work with the diagonal form of D_0 [5–7], and we proceed to define it:

$$D = U D_0 U^\dagger = K' \mathrm{e}^{\alpha J_z} \tag{8}$$

where

$$U = \exp[\mathrm{i}(\eta J_+ + \eta^* J_-)]\,. \tag{9}$$

The free energy can now be written as

$$\begin{aligned} \beta F &= \beta \operatorname{Tr}(U^\dagger D U H) + \operatorname{Tr}(D \ln D) \\ &= \beta \operatorname{Tr}(D U H U^\dagger) + \operatorname{Tr}(D \ln D)\,. \end{aligned} \tag{10}$$

The variational parameters are now the temperature, α and η. In fact, as far as the stationary properties of the system are concerned, it is enough to consider the imaginary part of η. We define

$$\eta = \theta/2\mathrm{i} \qquad \theta \text{ a real number}.$$

Explicitily one gets, for example

$$\begin{aligned} U^\dagger J_x U &= J_x \cos\theta - J_z \sin\theta \\ U^\dagger J_y U &= J_y \\ U^\dagger J_z U &= J_z \cos\theta + J_x \sin\theta\,. \end{aligned} \tag{11}$$

For the free energy we get

$$\begin{aligned} F = \epsilon \cos\theta \frac{N}{2} \tanh\left(\frac{\alpha}{2}\right) - (V+W)\sin^2\theta \frac{N}{4}(N-1)\tanh^2\left(\frac{\alpha}{2}\right) \\ + \frac{\alpha N}{2\beta}\tanh\left(\frac{\alpha}{2}\right) - \frac{N}{\beta}\ln\left[2\cosh\left(\frac{\alpha}{2}\right)\right] - \frac{WN}{2}\,. \end{aligned} \tag{12}$$

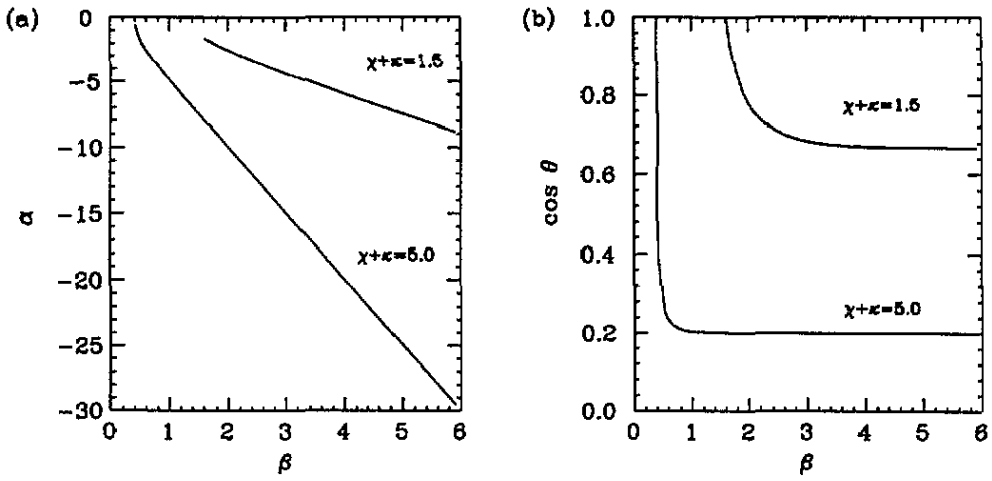

Figure 1. Relationship between the variational parameters α (a) as well as θ (b) and the inverse temperature β of the system in the *deformed phase* for two different values of coupling parameters sum $(\chi + \kappa)$. Note that this phase just exists for $(\chi + \kappa) \geqslant 1$.

We next consider that this quantity scales with N provided that we define

$$\chi = \frac{V(N-1)}{\epsilon} \tag{13}$$

$$\kappa = \frac{W(N-1)}{\epsilon}. \tag{14}$$

We can now take the limit $N \to \infty$ and calculate

$$\frac{\partial F}{\partial \theta} = -\epsilon \sin\theta \frac{N}{2} \tanh\left(\frac{\alpha}{2}\right) - \epsilon(\chi + \kappa) \sin\theta \cos\theta \frac{N}{2} \tanh^2\left(\frac{\alpha}{2}\right) = 0 \tag{15}$$

$$\frac{\partial F}{\partial \alpha} = \frac{N}{4}\left\{\epsilon \cos\theta - \epsilon(\chi + \kappa) \sin^2 \tanh^2\left(\frac{\alpha}{2}\right) + \frac{\alpha}{\beta}\right\} \cosh^{-2}\left(\frac{\alpha}{2}\right) = 0. \tag{16}$$

The above equations have two solutions, which correspond to the normal and deformed phases, respectively.

Normal phase:

$$\theta = 0 \tag{17}$$

$$\alpha = -\beta\epsilon. \tag{18}$$

Deformed phase:

$$\cos\theta = -\frac{\beta\epsilon}{\alpha} \tag{19}$$

$$\alpha = (\chi + \kappa)\beta\epsilon \tanh\left(\frac{\alpha}{2}\right). \tag{20}$$

The solutions of the equations (19) and (20) have to be found numerically. The relationship between α, θ, β and $(\chi + \kappa)$ is non-trivial, as can be seen in figures 1(a), (b).

Notice that in order to have the deformed solution two conditions have to be satisfied:

$$\chi + \kappa \geqslant 1 \qquad \text{and} \qquad 0 \leqslant T \leqslant T_{\text{cr}}$$

where T_{cr} corresponds to the solution of the trancendental equation

$$\tanh\left(\frac{\beta_{\text{cr}}\epsilon}{2}\right) = \frac{1}{(\chi+\kappa)} \qquad (\cos\theta = 1)\,.$$

The relationship between β_{cr} and $\chi + \kappa$ is shown in figure 2.

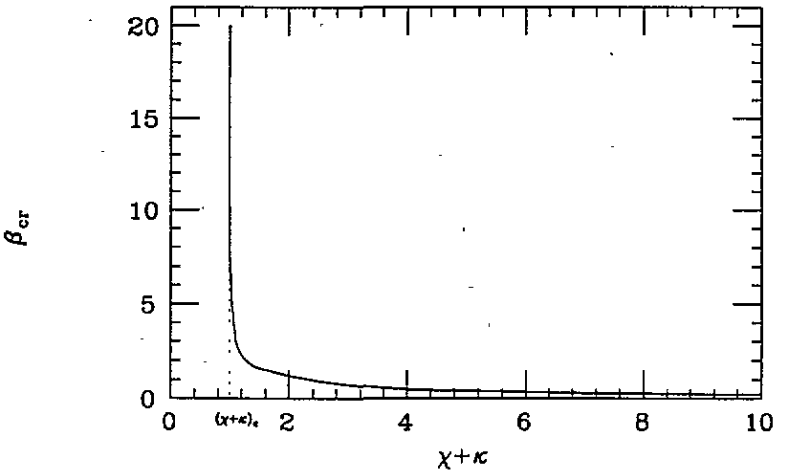

Figure 2. The critical inverse temperature, where the system changes phase, as a function of the coupling parameter sum $(\chi + \kappa)$. The critical value $(\chi + \kappa) = 1$ is indicated.

3.2. Thermodynamic properties and results

We are now in a position to calculate the following quantities as a function of the temperature.

The free energy

$$\bar{F} = \frac{F}{N} = \epsilon\frac{\cos\theta}{2}\tanh\left(\frac{\alpha}{2}\right) - \frac{\epsilon(\chi+\kappa)}{4}\sin^2\theta\tanh^2\left(\frac{\alpha}{2}\right) + \frac{\alpha}{2\beta}\tanh\left(\frac{\alpha}{2}\right) - \frac{1}{\beta}\ln\left[2\cosh\left(\frac{\alpha}{2}\right)\right]. \tag{21}$$

The internal energy

$$\bar{E} = \frac{\text{Tr}(DH')}{N\epsilon} = \frac{\cos\theta}{2}\tanh\left(\frac{\alpha}{2}\right) - \frac{(\chi+\kappa)}{4}\sin^2\theta\tanh^2\left(\frac{\alpha}{2}\right). \tag{22}$$

The entropy

$$\bar{S} = \frac{S}{k_{\text{B}}N} = -\frac{\text{Tr}(D\ln D)}{N} = -\frac{\alpha}{2}\tanh\left(\frac{\alpha}{2}\right) + \ln\left[2\cosh\left(\frac{\alpha}{2}\right)\right]. \tag{23}$$

The average density of excited particle

$$\bar{J}_z = \frac{\langle J_z\rangle}{N} = \frac{\cos\theta}{2}\tanh\left(\frac{\alpha}{2}\right). \tag{24}$$

The specific heat of the system

$$C = \frac{\partial E}{\partial T} = \frac{k_B \epsilon \beta^2}{4\cosh^2(\frac{\alpha}{2})}\left\{1 - (\chi+\kappa)\frac{\sin^2\theta}{\cos\theta}\tanh\left(\frac{\alpha}{2}\right)\right\}. \tag{25}$$

These four quantities are displayed in figures 3(*a*)–(*d*) for both the normal (broken curve) and the deformed phase (full curve). The specific heat is shown in figure 4 for three values of $(\chi+\kappa)$. The marked differences in both phases can be observed in all figures. Notice that for the normal phase the graphs are independent of $(\chi+\kappa)$. This can be easily understood from the above expressions, inserting the equilibrium solution $\theta = 0$. In the deformed case, the zero-temperature ground state has both levels populated, in contrast with the normal phase as can be seen by $\bar{J}_z$ in figure 3(*d*). For temperatures $\beta < \beta_{cr}$ the two solutions merge. The same physics is also reflected in the average energy (figure 3(*a*)) and free energy (figure 3(*c*)). The entropy shows an abrupt change for $\beta = \beta_{cr}$.

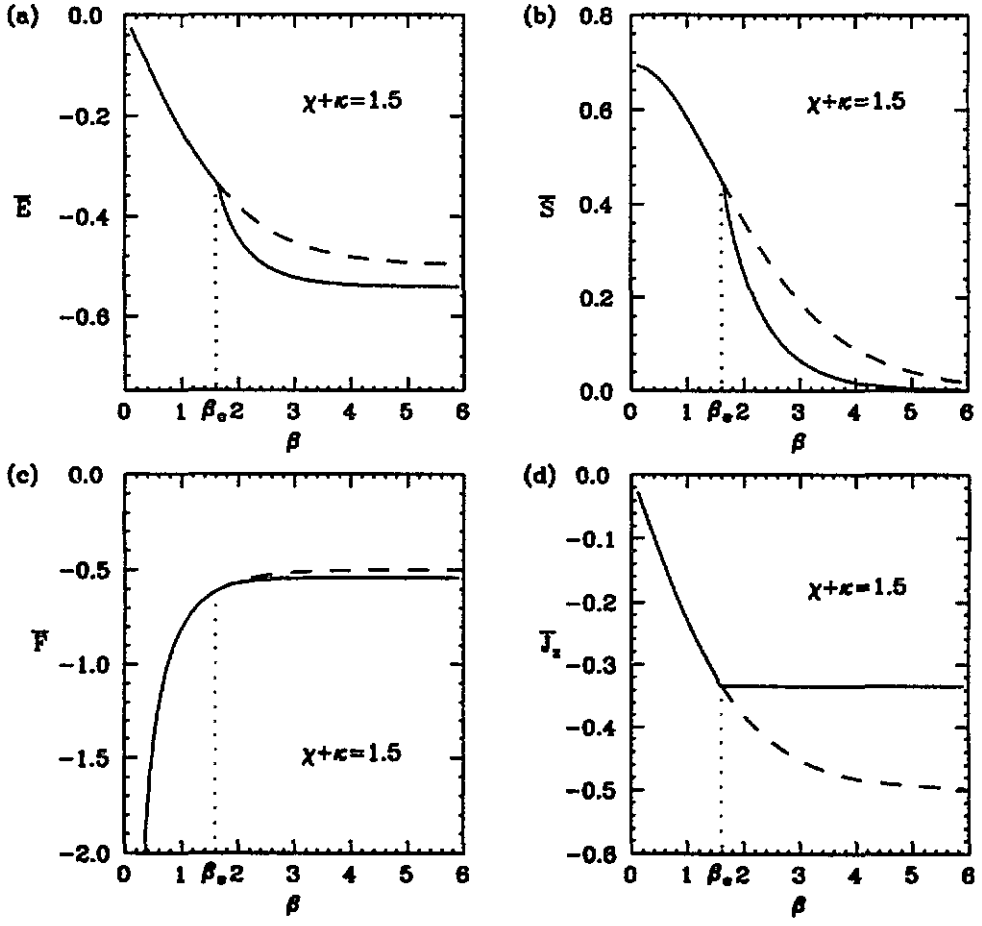

Figure 3. The internal energy $\bar{E}$ (*a*), the entropy $\bar{S}$ (*b*), the free energy $\bar{F}$ (*c*) and the average density of excited particles $\bar{J}_z$ (*d*) as a function of inverse temperature for $(\chi+\kappa) = 1.5$. The value of critical inverse temperature β_{cr} at which there is phase transition is shown and the two phases are separated by a vertical dotted line. The broken curves correspond to the normal phase. Its shape does not depend on coupling parameters, being a maximum of free energy for $(\chi+\kappa) \geqslant 1.0$ and the unique equilibrium solution for $(\chi+\kappa) \leqslant 1.0$, when there is no phase transition.

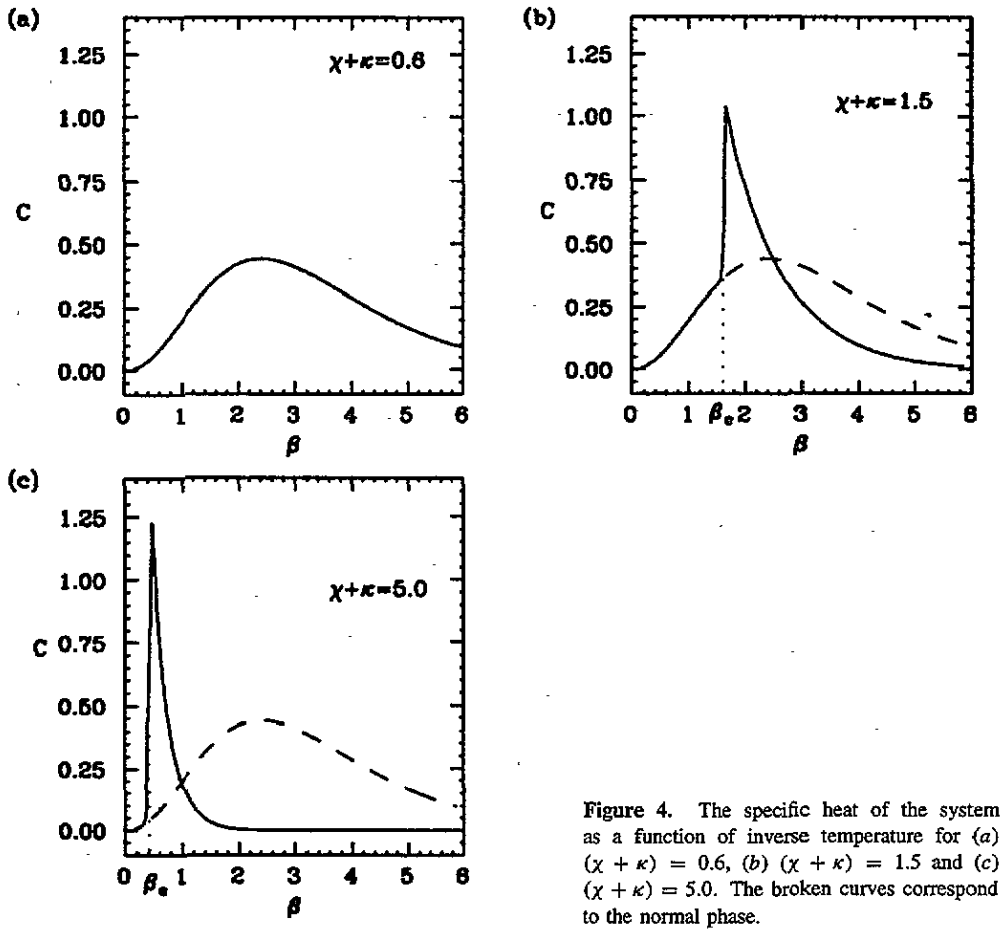

Figure 4. The specific heat of the system as a function of inverse temperature for (*a*) $(\chi + \kappa) = 0.6$, (*b*) $(\chi + \kappa) = 1.5$ and (*c*) $(\chi + \kappa) = 5.0$. The broken curves correspond to the normal phase.

4. Finite temperature dynamics

The following procedure to derive finite-temperature dynamics of the system is quite general and should be valid for all systems described in terms of generators of Lie groups. The method is presented in [5] and will be applied here to the $SU(2)$ Lipkin model.

4.1. Canonical variables and equations of motion

We start by constructing the thermal classical Lagrangian of the system ($\hbar = 1$),

$$L = \mathrm{i}\,\mathrm{Tr}(DU\dot{U}^{\dagger}) - \mathrm{Tr}(DUHU^{\dagger}) \tag{26}$$

where U has the same form as in the previous section, but with time-dependent parameters

$$U = \exp[\mathrm{i}(z(t)J_{+} + z^{*}(t)J_{-})] \tag{27}$$

and D is the equilibrium diagonal density (8).

In order to give an explicit expression for L, we need to calculate the following quantities:

$$\mathrm{Tr}(DU\dot{U}^{\dagger}) = -\frac{(z\dot{z}^{*} - \dot{z}z^{*})}{zz^{*}}\,(-\overline{J_z})\,\sin^2\sqrt{zz^{*}} \tag{28}$$

$$\mathrm{Tr}(DUJ_zU^\dagger) = \overline{J_z}\ \cos(2\sqrt{zz^*}) \tag{29}$$

$$\mathrm{Tr}(DU(J_+^2 + J_-^2)U^\dagger) = -(\overline{J_z})^2\ \frac{(N-1)}{N}\ \frac{z^{*2}+z^2}{zz^*}\ \sin^2(2\sqrt{zz^*}) \tag{30}$$

$$\begin{aligned}\mathrm{Tr}(DU(J_+J_- + J_-J_+)U^\dagger) &= 2\overline{J_z}\ \cos(2\sqrt{zz^*}) + 2\cos^4\sqrt{zz^*}(2\bar{J}_x^2 - \bar{J}_z)\\ &\quad + 8\sin^2\sqrt{zz^*}\cos^2\sqrt{zz^*}\ \overline{J_z^2} + 2\sin^4\sqrt{zz^*}(2\overline{J_x^2} + \overline{J_z})\end{aligned} \tag{31}$$

with $\overline{J_z} = \mathrm{Tr}(DJ_z) = (N/2)\tanh(\alpha/2)$ and $\overline{J_x^2} = \mathrm{Tr}(DJ_x^2) = N/4$.

We next look for a canonically conjugate pair of variables. Looking at (28) it is a simple matter to check that

$$\delta = z\ (-2\overline{\bar{J}_z})^{1/2}\ \frac{\sin\sqrt{zz^*}}{\sqrt{zz^*}} \tag{32}$$

$$\delta^* = z^*\ (-2\overline{\bar{J}_z})^{1/2}\ \frac{\sin\sqrt{zz^*}}{\sqrt{zz^*}} \tag{33}$$

are the canonically conjugate pair. In terms of δ and δ^* the Lagrangian can be written as

$$L = \frac{\mathrm{i}}{2}(\dot{\delta}\delta^* - \delta\dot{\delta}^*) - \epsilon(\bar{J}_z + \delta\delta^*) + \frac{1}{2}\frac{\epsilon\chi}{N}(\delta^2 + \delta^{*2})(2\bar{J}_z + \delta\delta^*) + \frac{\epsilon\kappa}{N}H_3 \tag{34}$$

where

$$H_3 = \overline{J_z} + \delta\delta^* + \left(1 + \frac{\delta\delta^*}{2\overline{\bar{J}_z}}\right)^2(2\overline{J_x^2} - \overline{J_z}) - 4\left(\frac{\delta\delta^*}{2\overline{\bar{J}_z}}\right)\left(1 + \frac{\delta\delta^*}{2\overline{\bar{J}_z}}\right)\overline{J_z^2} + \left(\frac{\delta\delta^*}{2\overline{\bar{J}_z}}\right)^2(2\overline{J_x^2} + \overline{J_z})\,. \tag{35}$$

The corresponding Hamiltonian can now be derived,

$$\frac{H}{\epsilon} = \overline{J_z} + \delta\delta^* - \frac{1}{2}\frac{\chi}{N}(\delta^2 + \delta^{*2})(2\bar{J}_z + \delta\delta^*) - \frac{\kappa}{N}H_3\,. \tag{36}$$

The range of allowed values for $\delta\delta^*$ is obtained from the condition

$$\cos^2\sqrt{zz^*} = 1 + \frac{\delta\delta^*}{2\bar{J}_z} \tag{37}$$

from which one gets

$$0 \leqslant \delta\delta^* \leqslant -2\bar{J}_z\,. \tag{38}$$

In terms of action and angle variables

$$\delta = \sqrt{-\bar{J}_z + I}\ \mathrm{e}^{\mathrm{i}\theta} \tag{39}$$

$$\delta^* = \sqrt{-\bar{J}_z + I}\ \mathrm{e}^{-\mathrm{i}\theta} \tag{40}$$

with $\bar{J}_z \leqslant I \leqslant -\bar{J}_z$.

The classical energy of the system can be rewritten as

$$E = \frac{H}{\epsilon J} = \eta + \tfrac{1}{2}(T_h^2 - \eta^2)(\chi\cos(2\theta) - \kappa) \tag{41}$$

where $\eta = I/J$, $T_h = \bar{J}_z/J = \tanh(\alpha/2)$ and the limitations on the phase space are given by

$$T_h \leqslant \eta \leqslant -T_h \tag{42}$$

$$-\pi \leqslant \theta \leqslant \pi\,. \tag{43}$$

For the sake of clarity we display T_h as a function of temperature in figures 5(*a*),(*b*). Notice from the above conditions that the size of the phase space shrinks as the temperature increases. This is a direct consequence of the relationship between η and $\bar{J}_z$. When $T \to \infty$ there will be only one configuration which minimizes the free energy, i.e. $\bar{J}_z = 0$. In the opposite limit, i.e. $T \to 0$ we get the result given in the literature [8].

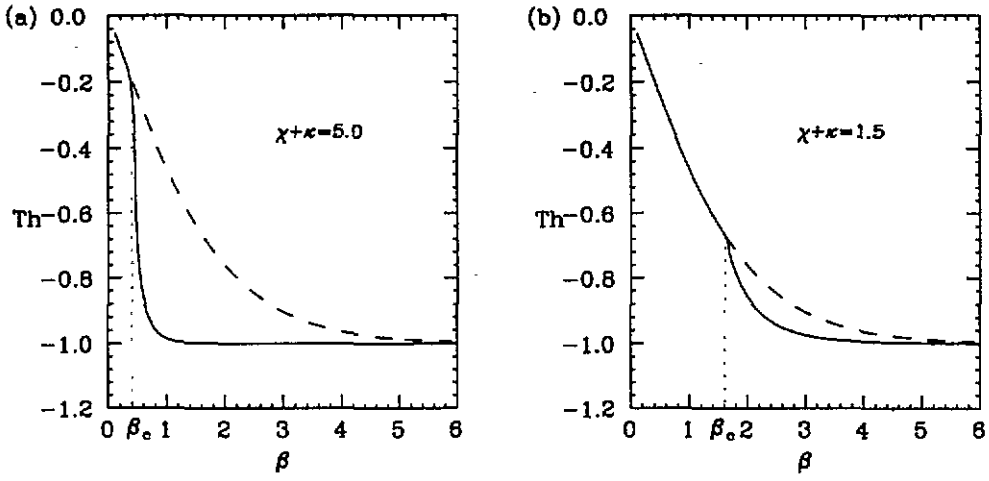

Figure 5. T_h as a function of inverse temperature β for two values of coupling parameters sum: (*a*) $(\chi + \kappa) = 5.0$ and (*b*) $(\chi + \kappa) = 1.5$. The broken curves correspond to coupling parameter sum below 1.0.

4.2. Fixed points and bifurcations

The equations of motion can now be calculated,

$$\dot{\eta} = -\frac{\partial E}{\partial \theta} = \chi(T_h^2 - \eta^2)\sin(2\theta) \tag{44}$$

$$\dot{\theta} = \frac{\partial E}{\partial \eta} = 1 - \eta[\chi\cos(2\theta) - \kappa]\,. \tag{45}$$

As we shall see in what follows the dynamics may exhibit three types of behaviour as a function of the relationship between the parameters χ and κ.

First case: $\chi = 0$ and $\kappa \neq 0$.

In this case for $\kappa > 1$ the effect of the interaction is to produce a line of minima which disappears as the temperature increases. This can be seen mathematically by the condition

$$\dot{\eta} = 0 \qquad \dot{\theta} = 0 = 1 + \eta\kappa \Longrightarrow \eta = -\frac{1}{\kappa} \quad \text{with} \quad |T_h| \geqslant \frac{1}{\kappa}. \tag{46}$$

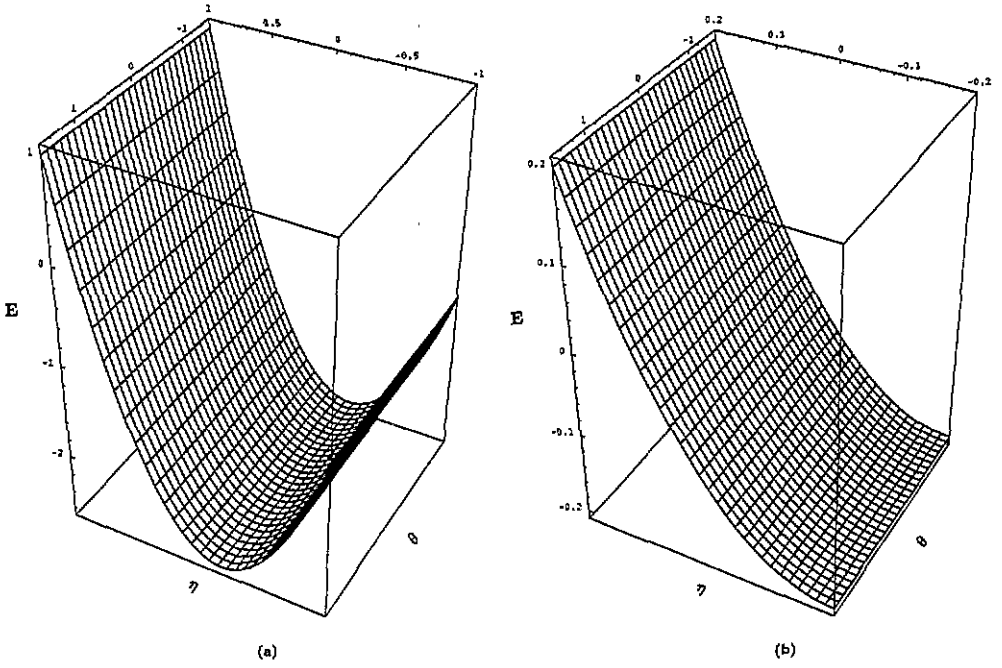

Figure 6. Classical energy surface $E(\eta, \theta)$ for intervals $+T_h \leqslant \eta \leqslant -T_h$, $-\pi/2 \leqslant \theta \leqslant \pi/2$ for coupling parameters $\kappa = 5.0$ and $\chi = 0.0$ (first case) for (*a*) $T_h = -1$ ($T = 0$) and (*b*) $T_h = -0.2$ ($T = T_{cr}$). Note the energy-range reduction, phase-space shrinkage and the disappearence of the line of minima at T_{cr}.

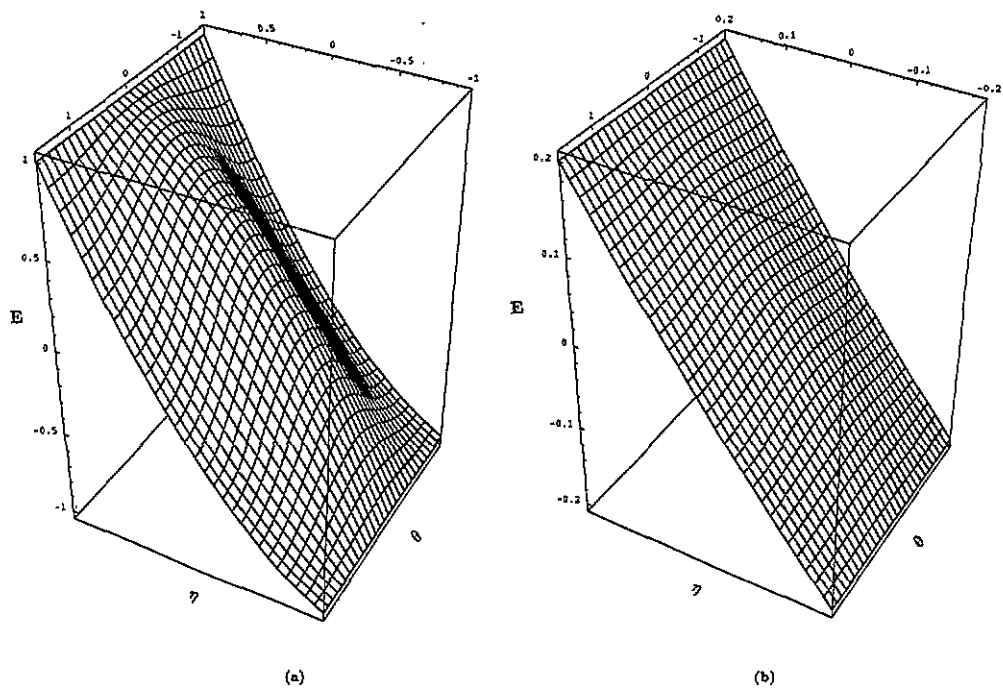

Figure 7. Classical energy surface $E(\eta, \theta)$ for intervals $+T_h \leqslant \eta \leqslant -T_h$, $-\pi/2 \leqslant \theta \leqslant \pi/2$ for coupling parameters $\chi = 0.6$ and $\kappa = 0.0$ (second case) for (*a*) $T_h = -1$ ($T = 0$) and (*b*) $T_h = -0.2$.

In figures 6(*a*), (*b*) the energy is depicted as a function of η and θ for $T = 0$ (*a*) and $T = T_{cr}$ (*b*). Notice that the critical temperature here, which corresponds to the disappearence of the line of minima, is precisely the one predicted by the thermodynamics of the model.

This bifurcation is intimately connected to the effect of temperature on the dynamics of the system that is to 'weaken' the contribution of the interaction term.

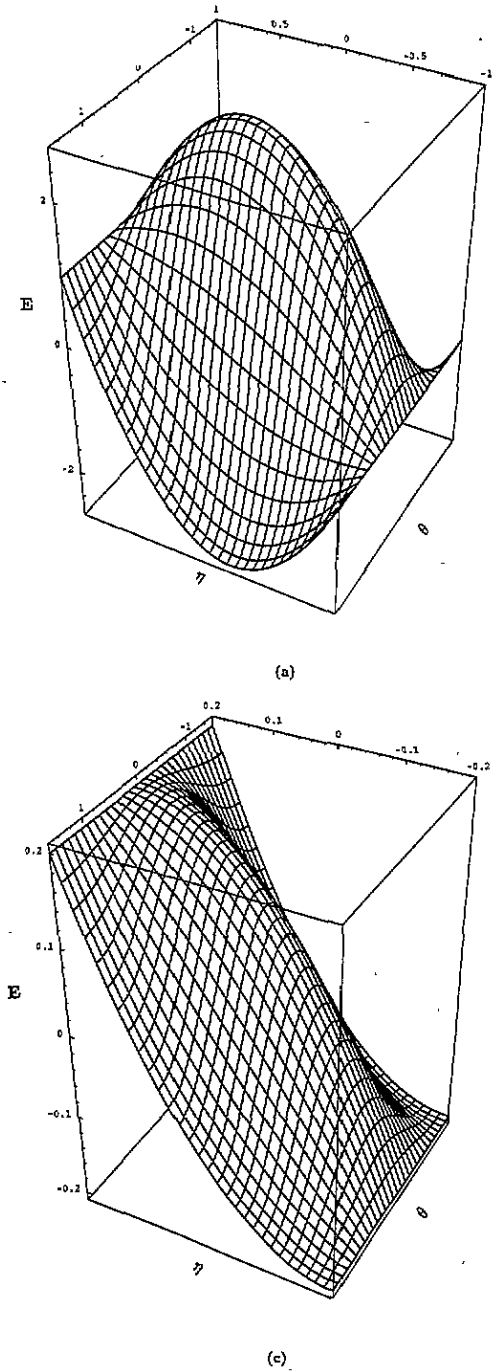

Figure 8. Classical energy surface $E(\eta, \theta)$ for intervals $+T_h \leqslant \eta \leqslant -T_h$, $-\pi/2 \leqslant \theta \leqslant \pi/2$ for coupling parameters $\chi = 5.0$ and $\kappa = 0.0$ (second case) for (*a*) $T_h = -1$ ($T = 0$), (*b*) $T_h = -0.5$ ($0 < T < T_{cr}$) and (*c*) $T_h = -0.2$ ($T = T_{cr}$). Note the disappearence of the closed orbits (libration) with temperature increase.

Second case: $\chi \neq 0$ and $\kappa = 0$.

The case $\chi < 1$ is very simple. There are no fixed points and all phase-space trajectories are open (rotation motion) (see figure 7(a)). The effect of temperature in this case is again shrinking phase space and flattening of the energy surface, which corresponds qualitatively to a weaker coupling.

The case $\chi > 1$ shows a bifurcation of equilibria where the following fixed points disappear as a function of the temperature (see figures 8(a)–(c)) and the corresponding contour lines on figures 9(a), (b):

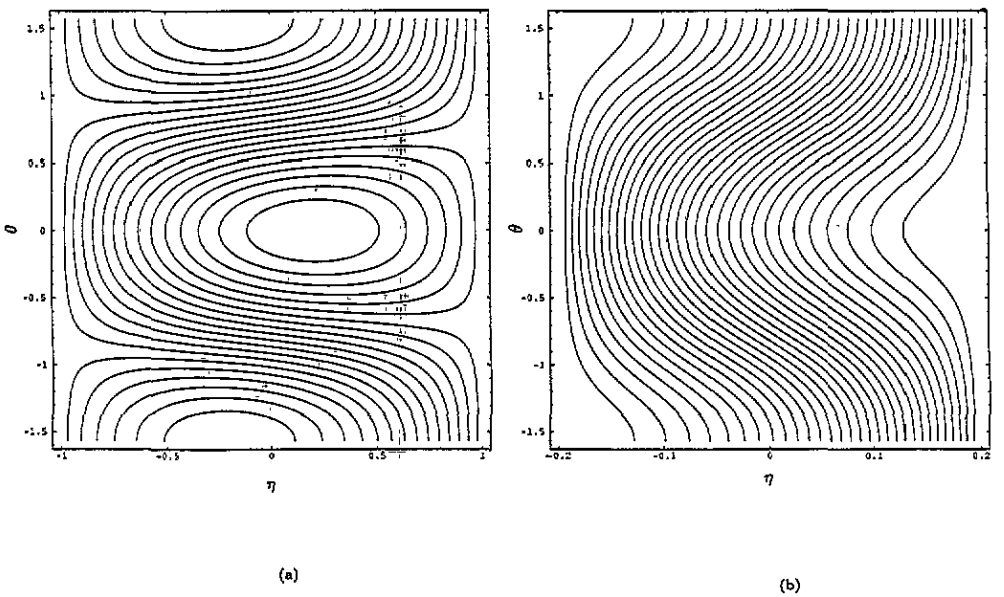

Figure 9. Contour lines corresponding to figure 8 energy surfaces at (a) $T_h = -1$ ($T = 0$) and (b) $T_h = -0.2$ ($T = T_{cr}$). At the phase transition temperature all the closed orbits disappear (libration) and we just have opened orbits (rotation) in the phase space.

(a) Two maxima

$$P_1 = \left(\frac{1}{\chi}, n\pi\right) \qquad n = 0, 1 \qquad \text{with energy} \quad E_1 = \frac{1 + T_h^2\chi^2}{2\chi}. \tag{47}$$

(b) Two minima

$$P_2 = \left(-\frac{1}{\chi}, -\frac{\pi}{2} + n\pi\right) \qquad n = 0, 1 \qquad E_2 = -E_1. \tag{48}$$

(c) Separatrix 1: four saddle points

$$P_3 = \left(T_h, \tfrac{1}{2}\cos^{-1}\left(\frac{1}{\chi T_h}\right) - n\pi\right) \qquad n = 0, 1 \qquad E_3 = T_h \tag{49}$$

$$P_4 = \left(T_h, -\tfrac{1}{2}\cos^{-1}\left(\frac{1}{\chi T_h}\right) + n\pi\right) \qquad n = 0, 1 \qquad E_4 = T_h. \tag{50}$$

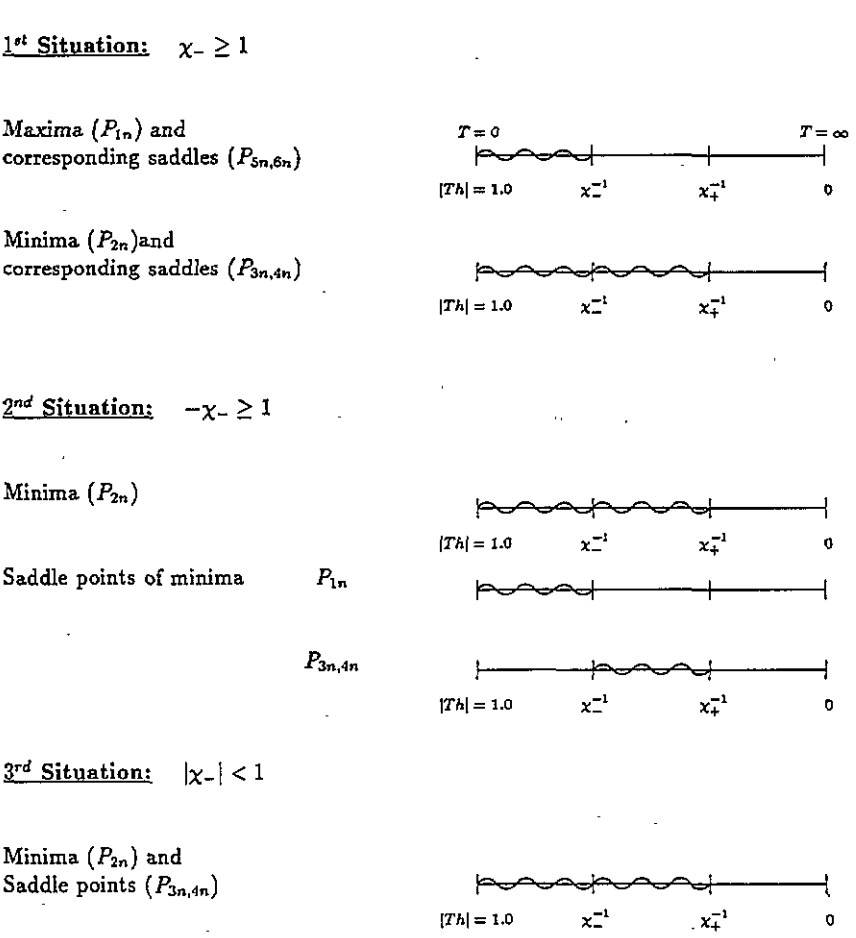

Figure 10. The three situations found in the third case as a function of the relationship of the coupling parameters χ and κ. The fixed points are presented with their range of existence marked with a wavy line.

(d) Separatrix 2: four saddle points

$$P_5 = \left(-T_h, \tfrac{1}{2}\cos^{-1}\left(\frac{-1}{\chi T_h}\right) - n\pi\right) \qquad n = 0, 1 \qquad E_5 = -T_h \tag{51}$$

$$P_6 = \left(-T_h, -\tfrac{1}{2}\cos^{-1}\left(\frac{-1}{\chi T_h}\right) + n\pi\right) \qquad n = 0, 1 \qquad E_6 = -T_h\,. \tag{52}$$

The energy surfaces for the situation discussed can be found in figures 6(*a*),(*b*) (first case), figures 7(*a*),(*b*) and 8(*a*)–(*c*) (second case), figures 11(*a*)–(*c*), 12(*a*),(*b*) and 13(*a*),(*b*) (third case).

Such points exist only for $T \leqslant T_{cr}$ where $T_h(T_{cr}) = -1/\chi$, the same temperature as obtained in the equilibrium case. Therefore, for the given ranges in T and χ, we get three

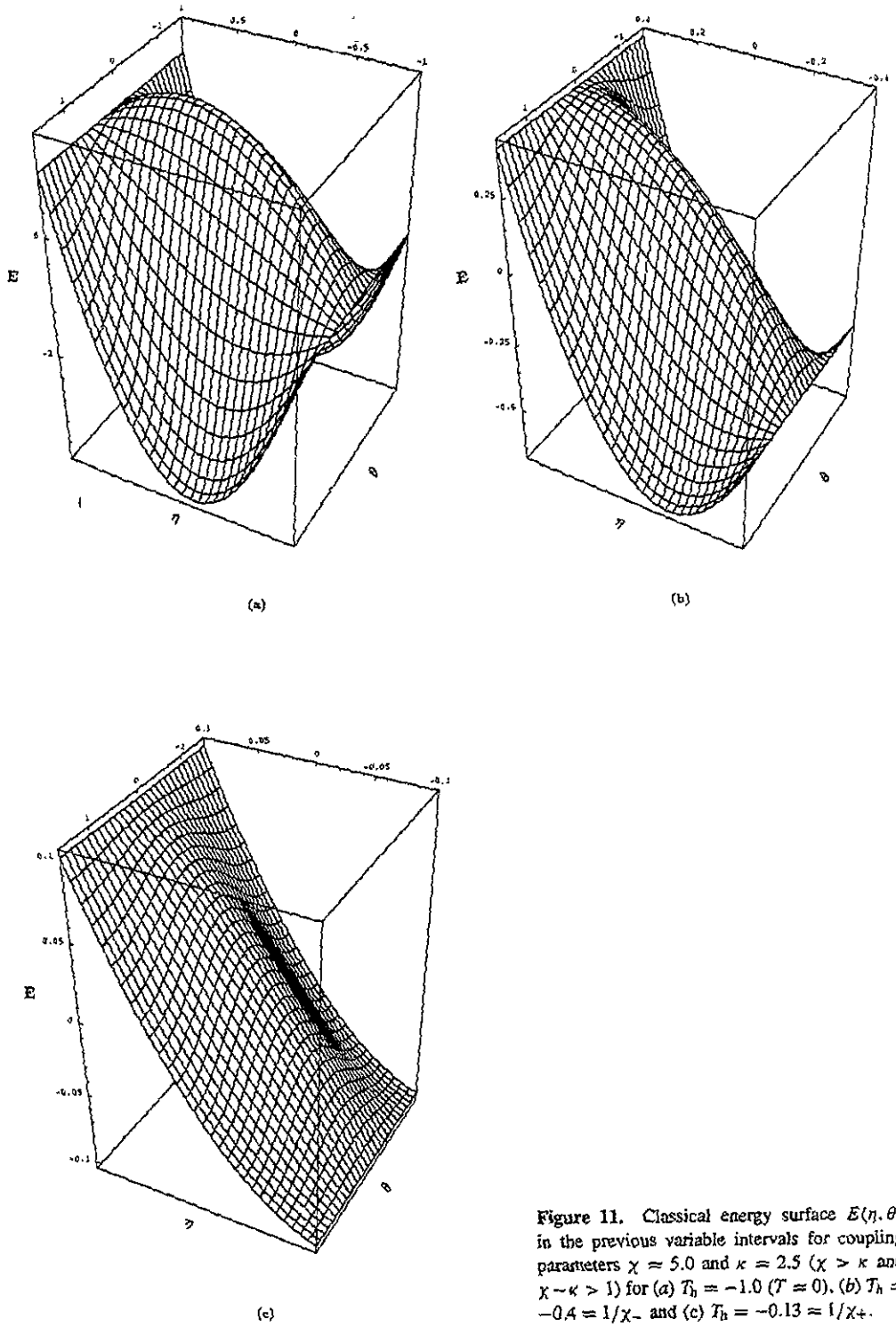

Figure 11. Classical energy surface $E(\eta, \theta)$ in the previous variable intervals for coupling parameters $\chi = 5.0$ and $\kappa = 2.5$ ($\chi > \kappa$ and $\chi - \kappa > 1$) for (*a*) $T_h = -1.0$ ($T = 0$), (*b*) $T_h = -0.4 = 1/\chi_-$ and (c) $T_h = -0.13 = 1/\chi_+$.

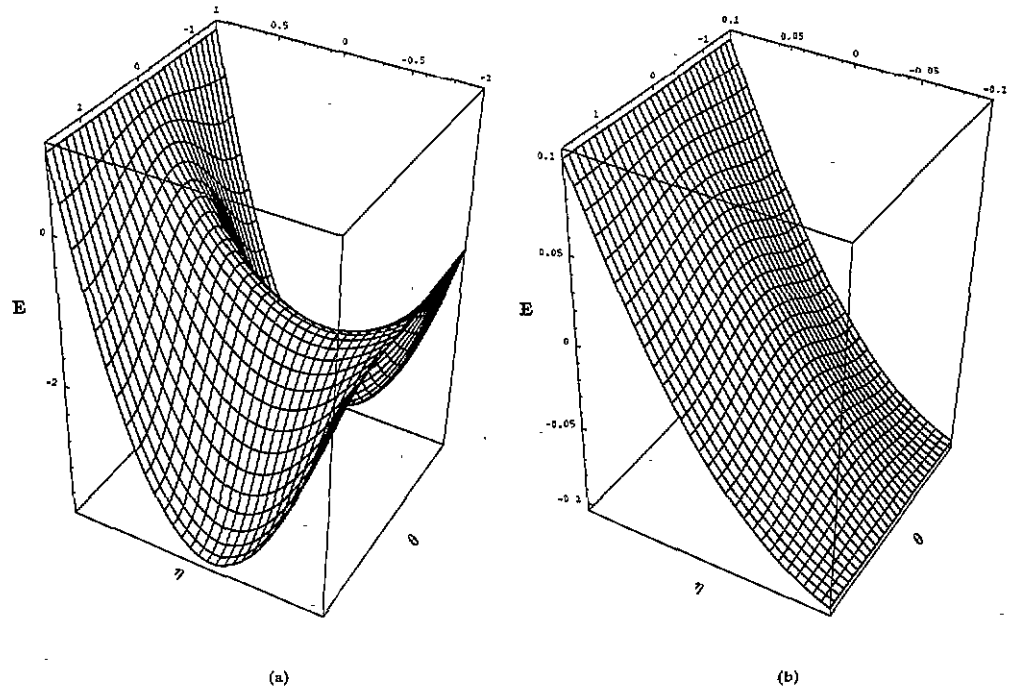

Figure 12. Classical energy surface $E(\eta, \theta)$ in the previous variable intervals for coupling parameters $\chi = 2.5$ and $\kappa = 5.0$ ($\chi < \kappa$ and $\kappa - \chi > 1$) for (*a*) $T_h = -1.0$ ($T = 0$), (*b*) $T_h = -0.13 = 1/\chi_+$.

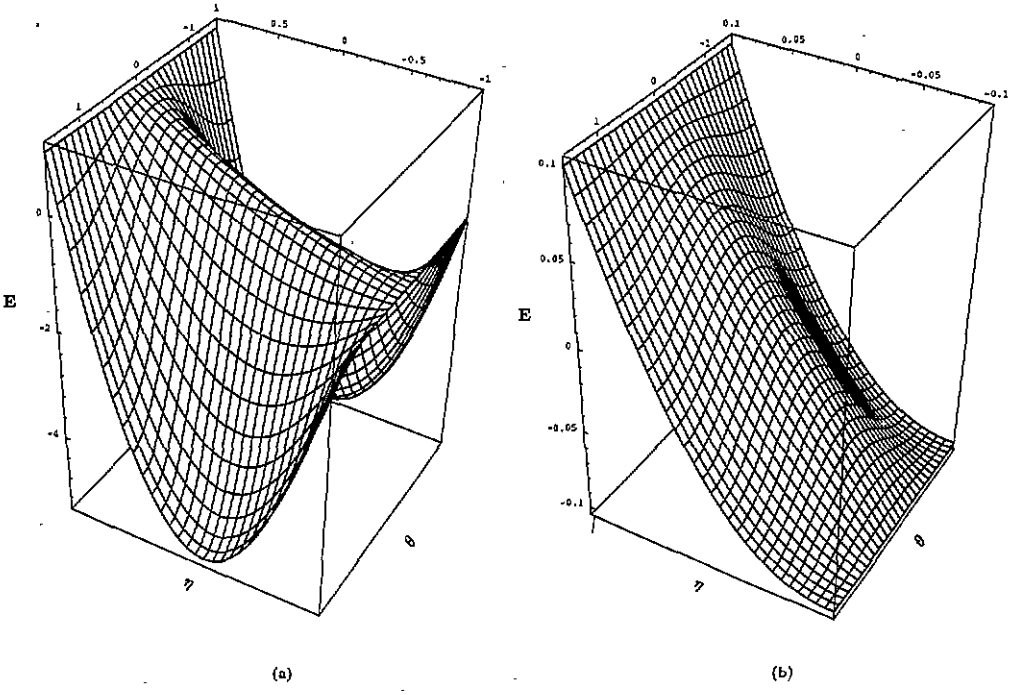

Figure 13. Classical energy surface $E(\eta, \theta)$ in the previous variable intervals for coupling parameters $\chi = 5.0$ and $\kappa = 5.5$ ($|\chi_-| < 1$) for (*a*) $T_h = -1.0$ ($T = 0$) and (*b*) $T_h = -0.1$.

Table 1. Energy, coordinates (η, θ), classification, range of validity an the range of temperature as function of the relationship of χ and κ of the twelve fixed points of the classical Hamiltonian (41) in the third case: $\chi \neq 0$ and $\kappa \neq 0$.

$(n = 0, 1)$	E	η	θ	Classification	Validity	Temperature range
				maxima	$\chi_- > 1$	
P_{1n}	$\dfrac{1+Th^2\chi_-^2}{2\chi_-}$	$\dfrac{1}{\chi_-}$	$n\pi$	or	or	$\lvert Th\rvert \geqslant \lvert\chi_-\rvert^{-1}$
				saddle points	$-\chi_- > 1$	
P_{2n}	$-\dfrac{1+Th^2\chi_+^2}{2\chi_+}$	$-\dfrac{1}{\chi_+}$	$-\dfrac{\pi}{2}+n\pi$	minima	$\chi_+ \geqslant 1$	$\lvert Th\rvert \geqslant \chi_+^{-1}$
					$\chi_- > 1$ or $\lvert\chi_-\rvert < 1$	$\lvert Th\rvert \geqslant \chi_+^{-1}$
$P_{\substack{3n\\4n}}$	Th	Th	$\pm\dfrac{1}{2}\cos^{-1}\left(\dfrac{1+\kappa Th}{\chi Th}\right)\mp n\pi$	saddle points	or	or
					$-\chi_- > 1$	$\chi_+^{-1} \leqslant \lvert Th\rvert \leqslant -\chi_-^{-1}$
$P_{\substack{5n\\6n}}$	$-Th$	$-Th$	$\pm\dfrac{1}{2}\cos^{-1}\left(\dfrac{-1+\kappa Th}{\chi Th}\right)\mp n\pi$	saddle points	$\chi_- > 1$	$\lvert Th\rvert \geqslant \chi_-^{-1}$

types of trajectories: a bounded motion (in η) around the maxima ($E > -T_h$) and minima ($E < T_h$) (*libration*) and an unbounded motion (in η) ($T_h \leqslant E \leqslant -T_h$) (*rotation*).

Third case: $\chi \neq 0$ and $\kappa \neq 0$.

In this case the parameters which determine the fixed points are the following combinations of χ and κ:

$$\chi_+ = \chi + \kappa \qquad \text{and} \qquad \chi_- = \chi - \kappa\,.$$

When $\chi_+ < 1$ no fixed points are found. When $\chi_+ \geqslant 1$, the fixed points with corresponding limits of validity are summarized in table **1**.

Qualitatively speaking we have three situations: they are schematized in figure 10. The range of existence is marked with a wavy line.

Notice that in all situations studied the effect of increasing temperature is to 'weaken' the coupling strength, in such a way that the system tends to situation $\chi = \kappa = 0$, as can be seen in figures 6(*b*), 7(*b*), 8(*c*), 11(*c*), 12(*b*) and 13(*b*).

5. Conclusions

In this work we have investigated both the thermodynamics and thermal dynamic properties of the $SU(2)$ Lipkin model. To our knowledge it is the first time that the originally proposed version of the model (with the interaction term in κ) has studied in such detail. Particular attention is given to the behaviour of fixed points and bifurcation of the equilibria with temperature. In our opinion the next interesting analysis to be performed is the thermal version of the $SU(3)$ Lipkin model where chaotic effects are also known to be present [9–12]. Work along this line is presently under way.

References

[1] Lipkin H J, Meshkov N and Glick J 1965 *Nucl. Phys.* **62** 188–98
[2] Kramer P and Saraceno M 1981 *Lecture Notes in Physics 140* (New York: Springer)
[3] Kan K K, Griffin J J, Licchtner P C and Dworzecka M 1979 *Nucl. Phys.* A **332** 109–24
[4] Yaffe L G 1982 *Rev. Mod. Phys.* **54** 407–35
[5] da Providência J and Fiolhais C 1985 *Nucl. Phys.* A **435** 190–204
[6] Yamamura Y, da Providência J and Kuriyama A 1990 *Nucl. Phys.* A **514** 461–70
[7] Yamamura Y, da Providência J, Kuriyama A and Fiolhais C 1989 *Prog. Theor. Phys.* **81** 1198–216
[8] Klauder J R and Skagerstam B S 1985 *Coherent States: Applications in Physics and Mathematical Physics* (Singapore: World Scientific)
[9] Meredith D C, Koonin S E and Zirnbauer M R 1988 *Phys. Rev.* A **39** 3499
[10] Lebouf P and Saraceno M 1990 *J. Phys. A: Math. Gen.* **23** 1745–64
[11] *Lebouf P and Saraceno M 1990 Phys. Rev.* A *41* 4614
[12] Lebouf P, Meredith D C and Saraceno M 1991 *Ann. Phys., NY* **208** 333–45